Homogeneous Catalysis

Direct Synthesis of Hydrogen Peroxide from Hydrogen and Oxygen by Using a Water-Soluble Iridium Complex and Flavin Mononucleotide**

Satoshi Shibata, Tomoyoshi Suenobu, and Shunichi Fukuzumi*

Hydrogen peroxide (H_2O_2) is known to be a highly selective and environmentally friendly oxidant and is used in the chemical industry for the manufacture of numerous organic and inorganic compounds.[1,2] However, the current industrial process for H_2O_2 production by sequential hydrogenation and oxidation of an alkyl anthraquinone is not environmentally benign as a result of a number of disadvantages, such as the requirement for toxic solvents, high energy consumption, and multiple steps.[3,4] To provide an alternative, extensive efforts have been devoted to achieving the direct synthesis of H_2O_2 from hydrogen (H_2) and oxygen (O_2) by using heterogeneous precious-metal catalysts (mainly Pd, Au, or Au–Pd).[3–12] This direct process suffers from serious problems such as unfavorable high-pressure conditions and relatively low yields owing to undesired side reactions such as formation of H_2O ($H_2 + \frac{1}{2}O_2 \rightarrow H_2O$), decomposition of H_2O_2 ($H_2O_2 \rightarrow H_2O + \frac{1}{2}O_2$), and hydrogenation of H_2O_2 ($H_2O_2 + H_2 \rightarrow 2 H_2O$).[3–12] For this reason, selectivity in the direct synthesis of H_2O_2 from H_2 and O_2 has been limited. In addition, it has been quite difficult to elucidate the heterogeneous catalytic mechanism as compared with the homogeneous catalytic mechanism, in which intermediates can be detected. However, there has to date been no report of a homogeneous catalytic system for the direct synthesis of H_2O_2 from H_2 and O_2.[13]

We report herein the direct synthesis of H_2O_2 from H_2 and O_2 in water by using a water-soluble iridium aqua complex [Ir^{III}(Cp*)(4-(1H-pyrazol-1-yl-κN^2)benzoic acid-κC^3)-(H_2O)]$_2$SO$_4$ ([1]$_2$SO$_4$), which can react with H_2 to produce an iridium hydride complex (**2**),[14,15] and flavin mononucleotide (FMN) under normal pressure and at room temperature. The synthesis and characterization of **1** were carried out as reported and are briefly described in the Experimental Section.[14]

At pH 6.0, the carboxylic acid group in **1** is deprotonated to give the carboxylate form **1-H$^+$** [Eq. (1)].[14] The Ir^{III}-OH$_2$

[*] S. Shibata, Dr. T. Suenobu, Prof. Dr. S. Fukuzumi
Department of Material and Life Science
Graduate School of Engineering, Osaka University
2-1 Yamada-oka, Suita, Osaka 565-0871 (Japan)
E-mail: fukuzumi@chem.eng.osaka-u.ac.jp
Homepage: http://www.etchem.mls.eng.osaka-u.ac.jp/
Prof. Dr. S. Fukuzumi
Department of Bioinspired Science, Ewha Womans University
Seoul 120-750 (Korea)

Supporting information for this article is available on the WWW under http://dx.doi.org/10.1002/anie.201307273.

complex **1-H$^+$** reacts with H_2 in an aqueous phosphate buffer solution (pH 6.0) to produce the iridium(III) hydride complex **2** ($\lambda_{max} = 336$ nm; Equation (2) and Figure 1).[14] The reaction of **1-H$^+$** with H_2 proceeds rapidly to completion to form **2** within 3 s (Figure S1 in the Supporting Information). For the
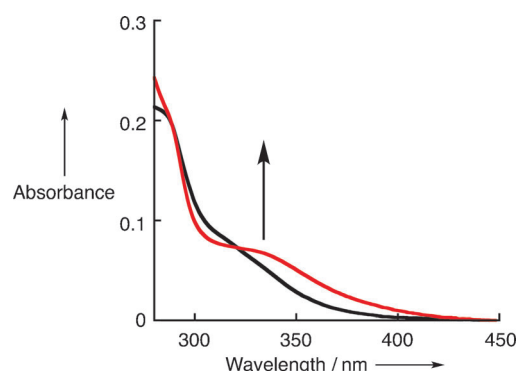

Figure 1. Changes in the UV/Vis absorption spectrum during the reaction of **1** (25 μm) with H_2 (0.82 mm) in an aqueous phosphate buffer (pH 6.0) at 298 K. An argon-saturated buffer solution of **1** (black line) was bubbled with H_2 (1.0×10^{-1} MPa) for 5 min thus resulting in the formation of **2** (red line).

reaction of **1-H$^+$** with H_2, the formation of **2** in the presence of O_2 was confirmed by changes in the UV/Vis absorption spectrum, which indicates the slower reaction of **2** with O_2 (Figure S2 in the Supporting Information).
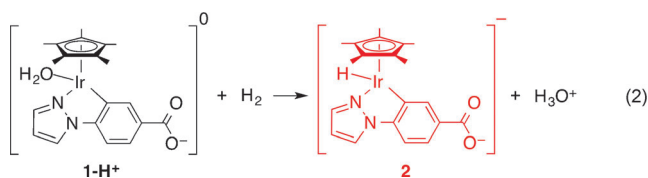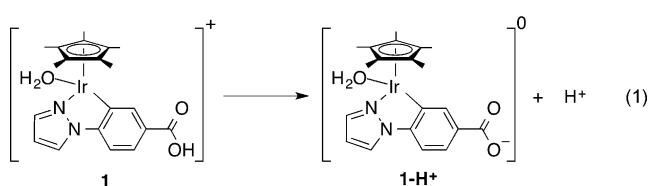
Complex **2** can efficiently reduce FMN ($\lambda_{max} = 373$ and 445 nm) to the 1,5-dihydroflavin (FMNH$_2$: $\lambda_{max} = 291$ nm and 390 nm) in aqueous phosphate buffer solution (pH 6.0) under N_2 [Equation (3) and Figure 2].[16] FMNH$_2$ was also generated by catalytic reduction of FMN with H_2 in the presence of

$$2 + \text{FMN} + H_3O^+ \longrightarrow \textbf{1-H}^+ + \text{FMNH}_2 \quad (3)$$
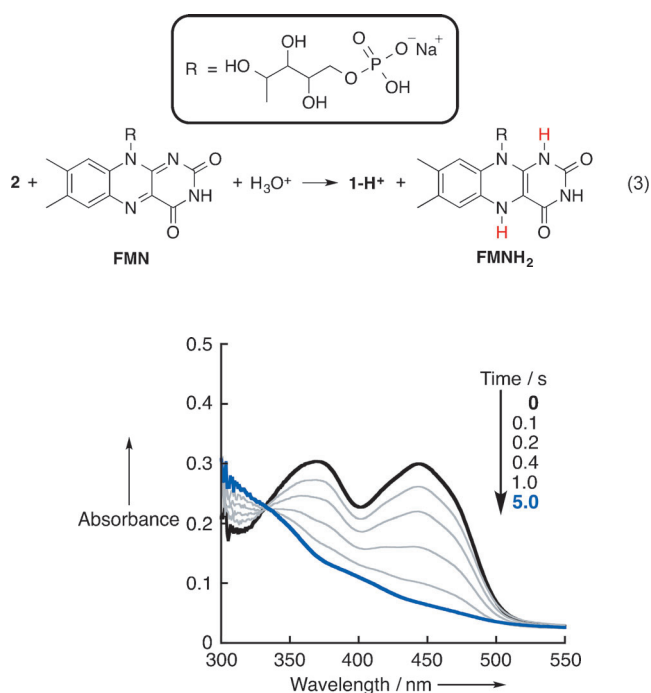

Figure 2. Changes in the UV/Vis absorption spectrum during the reduction of FMN (25 μM) by **2** (0.55 mM) under an H$_2$ (5.0×10^{-2} MPa)/N$_2$ (5.0×10^{-2} MPa) gas mixture after mixing a buffer solution of FMN (50 μM) under N$_2$ with that of **2**. Complex **2** was formed by the reduction of **1** (1.1 mM) by H$_2$ (bubbling for 10 min) under normal pressure in an aqueous phosphate buffer (pH 6.0) at 298 K. The black and blue solid lines correspond to FMN and FMNH$_2$, respectively.

1 (Figure S3 in the Supporting Information). A similar spectral change has been reported in the reaction of FMN with sodium dithionite in water.[15] The wavelengths (λ_{max}) and extinction coefficients at λ_{max} for the absorption spectrum of FMNH$_2$ obtained in this work ($\varepsilon = 3.6 \times 10^3 \, \text{M}^{-1}\text{cm}^{-1}$ at $\lambda_{max} =$ 390 nm) are consistent with those in the literature,[14] thus indicating the stoichiometric formation of FMNH$_2$. The decay of the absorption band of FMN at $\lambda_{max} = 445$ nm obeyed second-order kinetics (Figure S4a in the Supporting Information). Irrespective of the ratio of the initial amounts of **2** to FMN, the observed second-order rate constants (k_B) agree well with each other ($1.5 \times 10^5 \, \text{M}^{-1}\text{s}^{-1}$ and $1.2 \times 10^5 \, \text{M}^{-1}\text{s}^{-1}$, Figure S4a and b in the Supporting Information, respectively).

FMNH$_2$ can readily be oxidized by O$_2$ to regenerate FMN, accompanied by the formation of H$_2$O$_2$ [Eq. (4)].[17] Upon mixing an O$_2$-saturated phosphate buffer solution with

$$\text{FMNH}_2 + O_2 \longrightarrow \text{FMN} + H_2O_2 \quad (4)$$
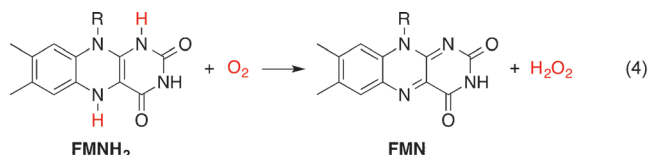
a buffer solution of FMNH$_2$ that was formed by the reduction of FMN by H$_2$ in the presence of **1**, the characteristic absorption bands of FMN were completely regenerated

(Figure 3). The rise of the absorption band of FMN at $\lambda_{max} = 445$ nm obeyed first-order kinetics (Figure S5 in the Supporting Information). From the slope of the first-order plot (inset of Figure S5 in the Supporting Information),
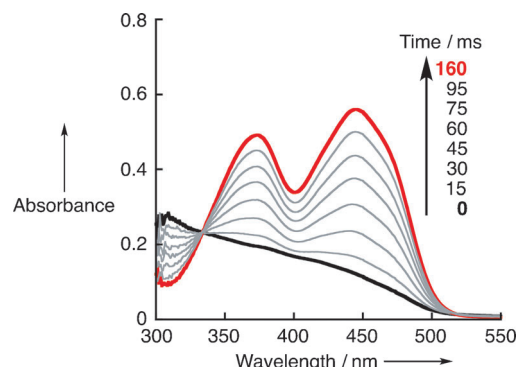

Figure 3. Changes in the UV/Vis absorption spectrum during the oxidation of FMNH$_2$ (50 μM) by O$_2$ (0.68 mM) under an O$_2$ (5.0×10^{-2} MPa)/N$_2$ (5.0×10^{-2} MPa) gas mixture in an aqueous phosphate buffer (pH 6.0) after mixing an O$_2$-saturated buffer solution with a buffer solution of FMNH$_2$ under N$_2$. FMNH$_2$ was formed in the reduction of FMN (100 μM) by H$_2$ (bubbling for 10 min) with **1** (5.0 μM) under normal pressure at 298 K.

a pseudo-first-order rate constant (k_{obs}) was obtained, and the second-order rate constant (k_C) for the reaction of FMNH$_2$ with O$_2$ was determined to be $2.0 \times 10^4 \, \text{M}^{-1}\text{s}^{-1}$.

FMNH$_2$ can also be independently generated by the reduction of FMN with sodium hydrosulfite (Na$_2$S$_2$O$_4$).[16a] As the reaction of FMNH$_2$ with O$_2$ proceeds, the formation of FMN leads to an increase in the absorbance at $\lambda_{max} = 445$ nm, and this increase obeyed first-order kinetics (Figure S6a in the Supporting Information). The pseudo-first-order rate constant (k_{obs}) proportionally increased with concentration of O$_2$ (Figure S6b in the Supporting Information). From the slope of the linear plot, the second-order rate constant for the reaction of FMNH$_2$ with O$_2$ was determined to be $2.8 \times 10^4 \, \text{M}^{-1}\text{s}^{-1}$. This value agrees well with k_C determined for the reaction in the presence of **1** and H$_2$. These values are more or less consistent with the value ($5.8 \times 10^4 \, \text{M}^{-1}\text{s}^{-1}$) reported for the reaction of a reduced form of a flavoprotein oxidase with O$_2$ at pH 7.0.[18]

The amount of H$_2$O$_2$ produced was determined by titration with the oxo[5,10,15,20-tetra(4-pyridyl)porphyrinato]titanium(IV) complex.[19] In the reaction consisting of the stepwise reduction of FMN by H$_2$ to form FMNH$_2$ when using **1** followed by the oxidation of FMNH$_2$ by O$_2$ to generate H$_2$O$_2$, a stoichiometric amount of H$_2$O$_2$ was produced when the concentration of FMN was varied, thus demonstrating a linear relationship between the concentrations of H$_2$O$_2$ and FMN with a slope of 1.0 (Figure 4).

Thus, the overall catalytic cycle for the selective direct synthesis of H$_2$O$_2$ from H$_2$ and O$_2$ by using **1** and FMN is expected to proceed according to Scheme 1: the iridium(III) complex **1-H**$^+$ reacts with H$_2$ to produce the Ir^{III}-H complex **2**, which reduces FMN to FMNH$_2$, followed by oxidation by O$_2$ to produce H$_2$O$_2$, accompanied by the regeneration of FMN.
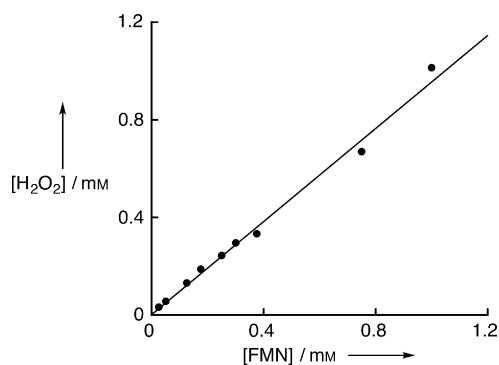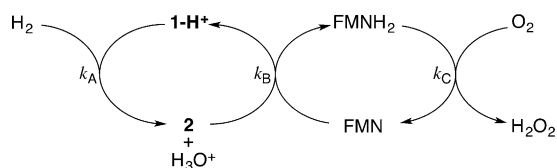
Figure 4. Plot of the concentration of H_2O_2 produced by the catalytic reduction of O_2 (1.0×10^{-1} MPa) by $FMNH_2$ (generated through the reduction of FMN by **2** under H_2) versus the concentration of FMN (25 μM–1.0 mM) loaded at the beginning of the reaction at 298 K. **2** was produced by the reduction of **1** (25 μM) by H_2 (1.0×10^{-1} MPa) in an aqueous phosphate buffer solution (pH 6.0).

Scheme 1.

When the catalytic reduction of FMN (5.0 μM) followed by the oxidation of $FMNH_2$ by O_2 was made possible by the presence of **1** (5.0 μM) in an aqueous phosphate buffer solution (pH 6.0), H_2O_2 was catalytically produced from H_2 and O_2. The formation of H_2O_2 stopped within a few minutes at pH 6.0 and 100 min at pH 2.8, when the turnover number (TON) of H_2O_2 production with respect to **1** and FMN reached 28 at pH 6.0 and 41 at pH 2.8 (Figure 5, black ●). This limited TON stands in sharp contrast to the stepwise catalytic reduction of FMN and the oxidation of $FMNH_2$ by O_2 (see above).
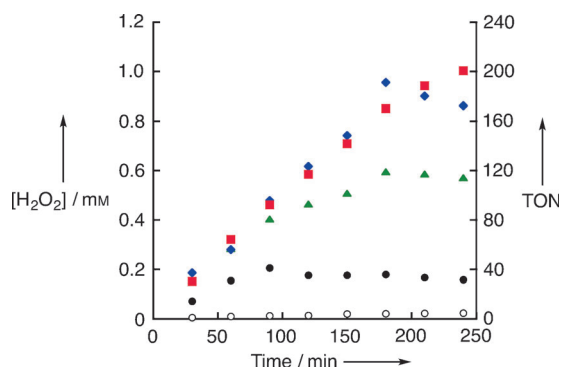

Figure 5. Time course of H_2O_2 production by the reaction of H_2 (5.0×10^{-2} MPa) with O_2 (5.0×10^{-2} MPa) catalyzed by **1** (5.0 μM) and FMN (5.0 μM) in water (pH 2.8) at 298 K in the absence (black ●) or presence of $Sc(NO_3)_3$ (25, 50, and 100 mM; green ▲, blue ◆, and red ■, respectively). Data shown by ○ were obtained in the absence of FMN but with **1** (5.0 μM) and $Sc(NO_3)_3$ (100 mM) under otherwise the same experimental conditions.

When $Sc(NO_3)_3$ (100 mM) was added to this system, the amount of H_2O_2 dramatically increased (Figure 5, red ■). The TON with respect to **1** and FMN reached 201 at 4 h. When **1** (1.0 μM) and FMN (50 μM) were used, the TON based on **1** reached 847 at 4 h. The product yield of H_2O_2 based on the total amount of H_2 and O_2 supplied in the catalytic reaction system was 19.2% at 10 min (Figure S7 in the Supporting Information). This value is more than three times larger than that obtained in the nanocolloidal Pd–Au system under normal pressure of a H_2/O_2 gas mixture (6.1%).[11d] The rate of catalytic formation of H_2O_2 is accelerated with $[Sc^{3+}]$ (Figure 5) and reached a turnover frequency (TOF) of 50 h^{-1}, however, the rate remained unchanged on increasing the concentration of Sc^{3+} over 50 mM. The limited TOF might be caused by the loss of H_2O_2 through the catalytic reduction of H_2O_2 by H_2 with **1** to produce H_2O (Scheme 2). This was independently confirmed by the reduction of H_2O_2 by H_2 when using **1** in water in the absence and presence of $Sc(NO_3)_3$ (Figure S8 in the Supporting Information).
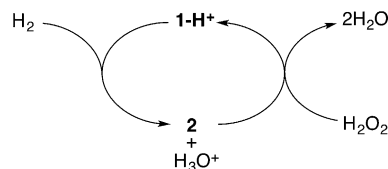
Scheme 2.

The reduction of H_2O_2 to H_2O by H_2 was catalyzed by **1** (Figure S8 in the Supporting Information, black ●). However, this reaction was effectively retarded by the presence of Sc^{3+} (Figure S8 in the Supporting Information, blue ◆ and red ▲), thus indicating that the further hydrogenation of H_2O_2 as shown in Scheme 2 could be inhibited by the presence of strong acid; a result consistent with the fact that H_2O_2 is known to be stabilized under acidic conditions.[20] In the same manner as in heterogeneous catalytic systems, the decomposition of H_2O_2 directly synthesized from H_2 and O_2 in reactions catalyzed by carbon- or TiO_2- supported Au, Pd, or an Au–Pd alloy was strongly retarded by the pretreatment of the catalyst with acid.[5a,c]

The rate-determining step of the catalytic scheme shown in Scheme 1 was investigated by examining the dependence of the overall rate of catalytic H_2O_2 production on the concentration of **1**. The rate of formation of H_2O_2 from H_2 and O_2 when using **1** in the presence of $Sc(NO_3)_3$ increased with increasing concentrations of **1** (Figure S9 in the Supporting Information), thus indicating that the rate-determining step is the reduction of FMN to $FMNH_2$ by **2** to regenerate **1**.[21] The characteristic UV/Vis absorption bands of FMN in the presence of **1** under N_2 (Figure S10a in the Supporting Information) remained unchanged under both H_2 and O_2 throughout the catalytic reaction (Figure S10b), thus indicating that FMN reduction by **2** is the rate-determining step of the overall catalytic reaction at pH 6.0. Under these conditions, selective two-electron reduction of O_2 to H_2O_2 occurs without the further reduction of H_2O_2 to H_2O.

In conclusion, the water-soluble iridium(III) complex **1** can efficiently catalyze the direct synthesis of H_2O_2 from H_2 and O_2 when using a water-soluble flavin (FMN) under normal pressure in aqueous solution at 298 K. The catalytic cycle consists of the reduction of **1** by H_2 to form the Ir^{III}-H complex **2**, followed by the reduction by **2** of FMN to $FMNH_2$, which then reacts with O_2 to produce H_2O_2, accompanied by the regeneration of FMN and **1**. The addition of $Sc(NO_3)_3$ led to a high TON (847) and a reasonably high yield of H_2O_2 (19.2%). This is because $Sc(NO_3)_3$ can inhibit the catalytic reduction of H_2O_2 by H_2 when using **1**.

Experimental Section

All experiments were performed under an Ar or N_2 atmosphere by using standard Schlenk techniques unless otherwise noted. The limiting concentration of O_2 in aqueous solution was prepared by using a mixed gas flow of O_2 and N_2 under normal pressure (1.0×10^{-1} MPa). The mixed gas was controlled by using a gas mixer (Kofloc GB-3C, KOJIMA Instrument Inc.), which can mix two or more gases at a defined partial pressure and mass flow rate. A defined concentration of H_2 in an aqueous solution was prepared by a mixed gas flow of H_2 and N_2 (or O_2) controlled by using a gas flow meter (KOJIMA Instrument Inc.) appropriate for each gas under normal pressure (1.0×10^{-1} MPa). UV/Vis absorption spectra were recorded on a Hewlett–Packard 8453 diode array spectrophotometer with a quartz cuvette (light-path length = 1 cm) at 298 K. Kinetic measurements for reactions with short half-lives (under 10 s) were performed on a UNISOKU RSP-601 stopped-flow spectrometer equipped with a MOS-type highly sensitive photodiode array at 298 K. Because the O_2/H_2 ratio is within the explosive range, dry catalyst should not be added to the O_2/H_2 gas mixture. Moreover, precautions should be taken to contain the system in the event of an explosion.

Details concerning chemicals, determination of the reaction yield, detection of H_2O_2, and pH adjustment are described in the Supporting Information.

[1] a) R. Hage, A. Lienke, *Angew. Chem.* **2006**, *118*, 212–229; *Angew. Chem. Int. Ed.* **2006**, *45*, 206–222; b) W. H. Hart, S. J. Hsieh, *Am. Inst. Chem. Eng. Symp.* **1998**, *319*, 73–76; c) B. S. Lane, K. Burgess, *Chem. Rev.* **2003**, *103*, 2457–2474; d) G. De Faveri, G. Ilyashenko, M. Watkinson, *Chem. Soc. Rev.* **2011**, *40*, 1722–1760.

[2] a) S. Fukuzumi, Y. Yamada, K. D. Karlin, *Electrochim. Acta* **2012**, *82*, 493–511; b) Y. Yamada, S. Yoshida, T. Honda, S. Fukuzumi, *Energy Environ. Sci.* **2011**, *4*, 2822–2825; c) R. S. Disselkamp, *Int. J. Hydrogen Energy* **2010**, *35*, 1049–1053.

[3] J. M. Campos-Martin, G. Blanco-Brieva, J. L. G. Fierro, *Angew. Chem.* **2006**, *118*, 7116–7139; *Angew. Chem. Int. Ed.* **2006**, *45*, 6962–6984.

[4] C. Samanta, *Appl. Catal. A* **2008**, *350*, 133–149.

[5] a) J. K. Edwards, B. Solsona, E. N. Ntainjua, A. F. Carley, A. A. Herzing, C. J. Kiely, G. J. Hutchings, *Science* **2009**, *323*, 1037–1041; b) J. K. Edwards, G. J. Hutchings, *Angew. Chem.* **2008**, *120*, 9332–9338; *Angew. Chem. Int. Ed.* **2008**, *47*, 9192–9198; c) J. K.

Edwards, E. N. Ntainjua, A. F. Carley, A. A. Herzing, C. J. Kiely, G. J. Hutchings, *Angew. Chem.* **2009**, *121*, 8664–8667; *Angew. Chem. Int. Ed.* **2009**, *48*, 8512–8515; d) E. N. Ntainjua, M. Piccinini, J. C. Pritchard, J. K. Edwards, A. F. Carley, J. A. Moulijn, G. J. Hutchings, *ChemSusChem* **2009**, *2*, 575–580; e) S. J. Freakley, M. Piccinini, J. K. Edwards, E. N. Ntainjua, J. A. Moulijn, G. J. Hutchings, *ACS Catal.* **2013**, *3*, 487–501; f) E. N. Ntainjua, S. J. Freakley, G. Hutchings, *Top. Catal.* **2012**, *55*, 718–722; g) E. N. Ntainjua, M. Piccinini, S. J. Freakley, J. C. Pritchard, J. K. Edwards, A. F. Carley, G. J. Hutchings, *Green Chem.* **2012**, *14*, 170–181.

[6] a) M. Sun, J. Zhang, Q. Zhang, Y. Wang, H. Wan, *Chem. Commun.* **2009**, 5174–5176; b) S. Park, S. H. Lee, S. H. Song, D. R. Park, S.-H. Baeck, T. J. Kim, Y.-M. Chung, S.-H. Oh, I. K. Song, *Catal. Commun.* **2009**, *10*, 391–394.

[7] Q. S. Liu, J. C. Bauer, R. E. Schaak, J. H. Lunsford, *Angew. Chem.* **2008**, *120*, 6317–6320; *Angew. Chem. Int. Ed.* **2008**, *47*, 6221–6224.

[8] a) G. B. Brieva, J. M. Campos-Martin, M. P. de Frutos, J. L. G. Fierro, *Catal. Today* **2010**, *158*, 97–102; b) G. Blanco-Brieva, M. P. D. Escrig, J. M. Campos-Martin, J. L. G. Fierro, *Green Chem.* **2010**, *12*, 1163–1166.

[9] J. Kim, Y.-M. Chung, S.-M. Kang, C.-H. Choi, B.-Y. Kim, Y.-T. Kwon, T. J. Kim, S.-H. Oh, C.-S. Lee, *ACS Catal.* **2012**, *2*, 1042–1048.

[10] T. García, R. Murillo, S. Agouram, A. Dejoz, M. Lázaro, L. Torrente-Murciano, B. Solsona, *Chem. Commun.* **2012**, *48*, 5316–5318.

[11] a) K. Mori, K. Furubayashi, S. Okada, H. Yamashita, *RSC Adv.* **2012**, *2*, 1047–1054; b) T. Deguchi, H. Yamano, M. Iwamoto, *J. Catal.* **2012**, *287*, 55–61; c) T. Ishihara, R. Nakashima, Y. Nomura, *Catal. Sci. Technol.* **2012**, *2*, 961–968; d) Y. Nomura, T. Ishihara, Y. Hata, K. Kitawaki, K. Kaneko, H. Matsumoto, *ChemSusChem* **2008**, *1*, 619–621; e) Q. Chen, E. J. Beckman, *Green Chem.* **2007**, *9*, 802–808.

[12] a) J. Xu, L. Ouyang, G.-J. Da, Q.-Q. Song, X.-J. Yang, Y.-F. Han, *J. Catal.* **2012**, *285*, 74–82; b) Y.-F. Han, Z. Zhong, K. Ramesh, F. Chen, L. Chen, T. White, Q. Tay, S. N. Yaakub, Z. Wang, *J. Phys. Chem. C* **2007**, *111*, 8410–8413.

[13] In homogeneous catalytic systems for the reaction of H_2 with O_2, no formation of H_2O_2 has been confirmed, see: a) Z. M. Heiden, T. B. Rauchfuss, *J. Am. Chem. Soc.* **2007**, *129*, 14303–14310; b) L. Vaska, M. E. Tadros, *J. Am. Chem. Soc.* **1971**, *93*, 7099–7101, whereas, a small amount of H_2O_2 was qualitatively detected, see: c) A. S. Berenblyum, A. G. Knizhnik, S. L. Mund, I. I. Moiseev, *J. Organomet. Chem.* **1982**, *234*, 219–235.

[14] a) Y. Maenaka, T. Suenobu, S. Fukuzumi, *J. Am. Chem. Soc.* **2012**, *134*, 367–374; b) Y. Maenaka, T. Suenobu, S. Fukuzumi, *Energy Environ. Sci.* **2012**, *5*, 7360–7367; c) Y. Maenaka, T. Suenobu, S. Fukuzumi, *J. Am. Chem. Soc.* **2012**, *134*, 9417–9427.

[15] A water-soluble Ir^{III} porphyrin was reported to react with H_2 to produce the corresponding iridium(III) hydride complex, see: a) S. Bhagan, B. B. Wayland, *Inorg. Chem.* **2011**, *50*, 11011–11020; b) S. Bhagan, G. H. Imler, B. B. Wayland, *Inorg. Chem.* **2013**, *52*, 4611–4617.

[16] a) A. S. Eisenberg, J. P. M. Schelvis, *J. Phys. Chem. A* **2008**, *112*, 6179–6189; b) Z. Shi, J. M. Zachara, L. Shi, Z. Wang, D. A. Moore, D. W. Kennedy, J. K. Fredrickson, *Environ. Sci. Technol.* **2012**, *46*, 11644–11652.

[17] a) S. Fukuzumi, S. Kuroda, T. Tanaka, *J. Am. Chem. Soc.* **1985**, *107*, 3020–3027; b) S. Fukuzumi, K. Tanii, T. Tanaka, *Chem. Commun.* **1989**, 816–818.

[18] J. Sucharitakul, M. Prongjit, D. Haltrich, P. Chaiyen, *Biochemistry* **2008**, *47*, 8485–8490.

[19] C. Matsubara, N. Kawamoto, K. Takamura, *Analyst* **1992**, *117*, 1781–1784.

[20] Hydrogenation was reported to be a major pathway for H_2O_2 decomposition on Pd or Pd–Au alloy supported on SBA-15, see: N. Gemo, P. Biasi, P. Canu, F. Menegazzo, F. Pinna, A. Samikannu, K. Kordás, T. O. Salmi, J.-P. Mikkola, *Top. Catal.* **2013**, *56*, 540–549.

[21] The maximum rate of this reaction step ($r_{B,max}$) in Scheme 1 under catalytic reaction conditions in the absence of $Sc(NO_3)_3$ was determined to be $r_{B,max} = k_B[FMN]_{max}[\mathbf{2}]_{max} = 1.5 \times 10^5 (M^{-1}s^{-1}) \times 5.0 \times 10^{-6} (M) \times 5.0 \times 10^{-6} (M) = 3.8 \times 10^{-6} M\,s^{-1}$. This value is significantly smaller than that for the next catalytic step ($r_{C,max}$), the reduction of O_2 by $FMNH_2$, which was determined to be $r_{C,max} = k_C[FMNH_2]_{max}[O_2] = 2.8 \times 10^4 (M^{-1}s^{-1}) \times 5.0 \times 10^{-6} (M) \times 1.4 \times 10^{-3} (M) = 2.0 \times 10^{-4} M\,s^{-1}$. The reaction rate of the first catalytic step (r_A), the reaction of **1** with H_2, can be evaluated based on the data in Figure S1 in the Supporting Information, and was determined to be $r_A > 6.0 \times 10^{-6} M\,s^{-1} > r_{B,max}$.